Chapter 4:

Optical and Transport Characteristic of $InBi_{1-x}Te_x$ Crystals

4.1 Introduction:

The most important research in both theoretical and experimental fields pertains to the optical properties of solid materials, including reflection, absorption, transmission, and the pertinent optical constants. These investigations have led to the discovery of extremely beneficial optical properties for construction of sophisticated multilayer optical devices. The advance knowledge of optical properties and material attributes are useful for both the research and commercial objectives. Additionally, these optical studies are particularly beneficial for understanding the electronic structure of solids. The results of optical studies can be used to very precisely determine the electronic energy band structures of semiconducting substances.

There are several known techniques for evaluating optical constants. The most significant of these are Abbe's method, optical spectroscopy method, critical angle method and polarimetric method [1-4]. However, the spectroscopic method is the one that is most frequently used. Particularly, optical absorption spectroscopy is the quickest, easiest and most direct technique for studying band structure. It is almost a need.

4.2 IR Analysis and Band gap:

A valence band electron is stimulated into the conduction band when a photon impinges on a semiconductor and has energy of the order of the band gap of the semiconductor or above. In contrast to the conduction band where most of the band states are empty and only a small number of states at its bottom are inhabited, the valence band states are virtually totally occupied. Due to the abundance of unoccupied states in the conduction band that an excited electron can occupy when it transits from its valence band state, the likelihood of this happening is significant. When an electron is excited to the conduction band by optical absorption, it may gain more energy than conduction band electrons, which almost all occupy states around Ec, the conduction band edge (figure 4.1). If the semiconductor is heavily doped, this may not be possible. However, this normally not the case. In order to achieve thermal equilibrium with the other pre-existing electrons in the conduction band, the excited electron would frequently release excess energy that it had accumulated through its lattice interaction, namely electron phonon scattering. The electron-hole pairs, which are formed by the migrated electrons in the conduction band and the vacant states (holes) they left in the valence band, act as additional charge carriers for conduction. As a result, extra carriers that are so produced are out of balance with the environment and eventually tend to recombine. The extra carriers, which are holes in the valence band and electrons in the conduction band, are readily available for electrical conduction because they are in their respective conductive bands. This undoubtedly raises conductivity.

Valence band electrons cannot be excited to the conduction band if the incident photon energy is smaller than the band gap. Therefore, excitation in pure semiconductors becomes more challenging in the absence of impurity levels in the band gap, leading to little or no photon absorption. Because of this, some substances are transparent in specific incident photon wavelength ranges, enabling us to "see through" insulators, like rock salt and ionic crystals, having sufficiently large energy band gaps that allow optical photons to travel through them. The visible range also penetrates through at photon energies above 2eV, generally at 3eV and higher. When a photon beam of energy more than the band gap is incident on the semiconductor, there will be absorption exhibited by the resulting spectrum. Both the sample thickness and the energy of the input photons affect how much relative intensity is absorbed. The relation given below can be used to determine the percentage of incident intensity that is transmitted:

$$I = I_0 e^{-\alpha t} \text{----- (4.1)}$$

where, α being the absorption coefficient (characteristic of the material), I_0 the incident intensity and I the transmitted intensity. The absorption coefficient α near the absorption edge of the spectrum can be expressed in terms of the band gap energy E_g [5] as:

$$\propto = A(h\nu - Eg)^{\gamma} \text{ ----(4.2)}$$

where, hυ is the photon energy (familiar expression), γ is a numerical constant which equals $\frac{1}{2}$ and $\frac{3}{2}$ for allowed and forbidden direct transitions, respectively.

In the literature a few reports are to be found on the optical characterization of single crystals of $InBi_{1-x}Se_x$ [14]. Optical absorption study on horizontal directional solidification (HDS) grown crystals of $InBi_{1-x}Sb_x$ has been reported by Ajaykumar [6].The report suggests that the material is low band gap, so author has chosen the FTIR method to obtain band gap.

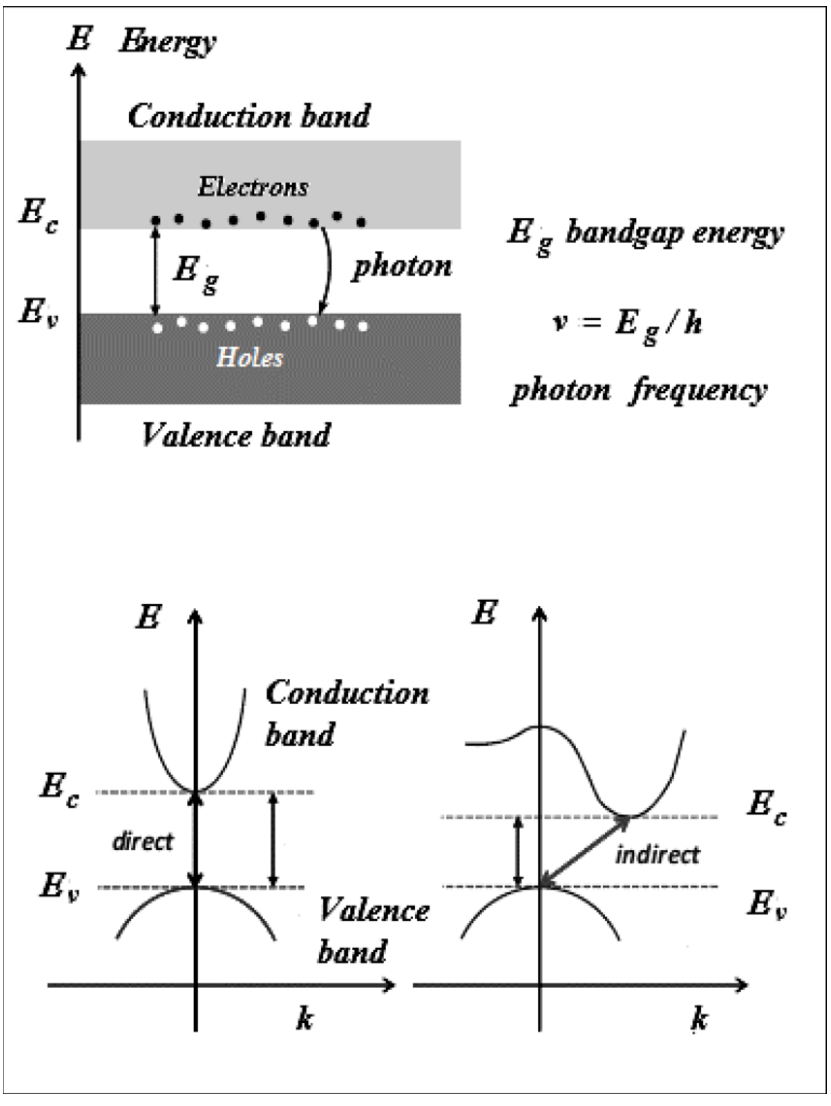

Figure 4.1: Band Structure

Experimental Discussion:

Radiation that ranges from 700 to 1000 nm is considered infra-red. The wave number unit cm^{-1} is used in the context of infrared spectrum. For infrared detection, the material should exhibit narrow band gap of at least less than 1.6 ev. It is useful to divide the infrared region into three sections: near, mid and far infrared. In table 4.1 indicate that range of spectrum in terms of wave length and wave number.

Table 4.1 Wavelength and Wave number for IR Region

Region	**Wavelength range** (nm)	**Wave number range** (cm^{-1})
Near	0.78 - 2.5	12800 – 4000
Middle	2.5 – 50	4000 – 200
Far	50 -1000	200 – 10

The most useful IR region lies between 4000–6700 cm^{-1}. There isn't enough energy in IR to induce electronic transitions, unlike ultraviolet radiation. IR is only absorbed by compounds with small vibrational and rotational energy differences. Atomic dipole moments must change within a molecule during vibration or rotation to allow a molecule to absorb IR. Dipole moments of atoms/molecules are affected by fluctuations in the alternating electrical field of radiation. In this case, radiation will change the amplitude of molecular vibration when the frequency of the radiation matches the vibrational frequency of the molecule.

To form crystal pellets, spectroscopic grade dry KBr powder at less than 5% concentration was thoroughly mixed with fine crystalline powder and formed into a 1 cm diameter palette, using a vacuum pelletizer. This experiment measured the optical absorption spectra in the 400 cm^{-1} to 4000 cm^{-1} wave number range. A spectrum analysis was performed to calculate the absorption coefficient based on photon energy. The relation between absorption coefficient (α) and the incident photon energy (E) near the absorption edge is expressed as

$$\boldsymbol{\alpha = A(E - Eg)^n} \text{ ---- (4.3)}$$

where A is varying function which may be regarded as a constant over narrow range considered and n is a number representing the nature of the transition. Several authors have investigated the phenomenon of optical absorption and the resulting interband transition. As a result, for the permitted direct transition, the absorption coefficient α near the absorption edge is proportional to the band gap E_g as $(\alpha h\upsilon)^2$ vs $(h\upsilon - E_g)$, where hυ is the incident photon energy [7-10]. Thus the plot of (αhυ) vs (hυ) is expected to be linear near the absorption edge .

The plots of $(\alpha h\upsilon)^2$ vs hυ were used to evaluate the optical band gaps. These plots are shown in Fig. 4.2 to 4.4 for $InBi_{1-x}Te_x$ (x = 0.05, 0.1, and 0.15). Near the fundamental absorption edge, the plots appear linear in the region of strong absorption. Hence by extrapolating the linear portion to $(\alpha h\upsilon)^2 = 0$, the band gap was evaluated. Since, the conduction band minimum lies lower than valence band maximum InBi compounds reflect semi-metallic character with an inverted band gap [11, 12]. The impurity Te atoms incorporated in the host InBi lead to bond length variations and shift of Fermi level. Due to these processes, more charge carriers will be created in the valence band, which give rise to semiconducting behavior [13,14]. A monotonic increase in band gap with Te concentration in InBi is observed (Figure- 4.5). The values of the band gap obtained are given in Table 4.2**.**

Table-4.2 Bandgap of $InBi_{1-x}Te_x$ (x=0.05,0.10 and 0.15) crystals

Crystal	**Bandgap (eV)**
$InBi_{0.95}Te_{0.05}$	0.195
$InBi_{0.90}Te_{0.10}$	0.213
$InBi_{.085}Te_{.015}$	0.232

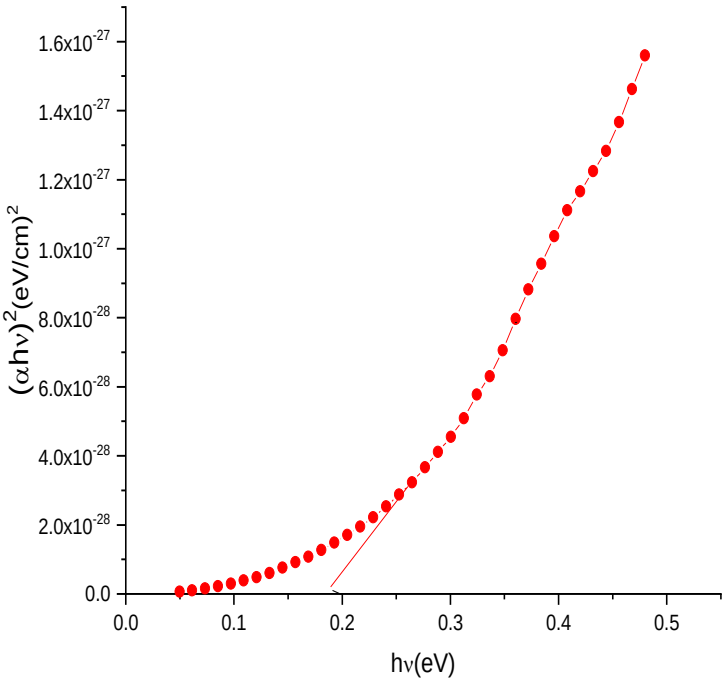

Figure 4.2: Plot of $(\alpha h\upsilon)^2$ vs hυfor $InBi_{0.95}Te_{0.05}$ crystal

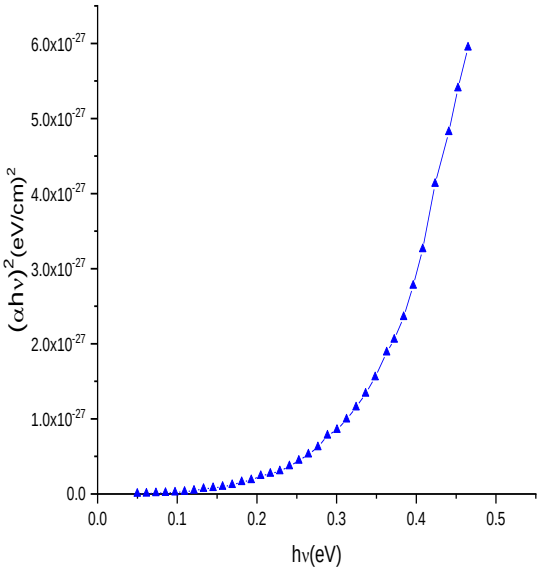

Figure 4.3: Plot of $(\alpha h\upsilon)^2$ vs hυ for $InBi_{0.90}Te_{0.10}$ crystal

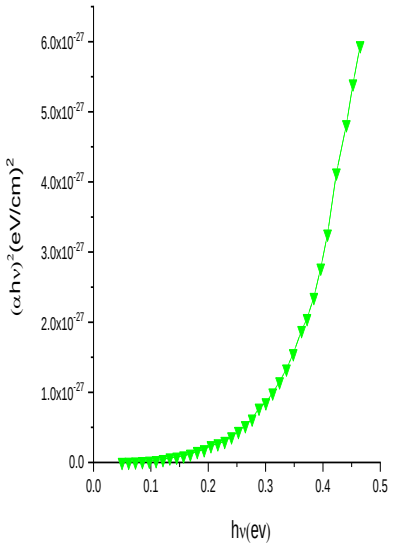

Figure 4.4: Plot of $(\alpha h\upsilon)^2$ vs hυ for $InBi_{0.85}Te_{0.15}$ crystal

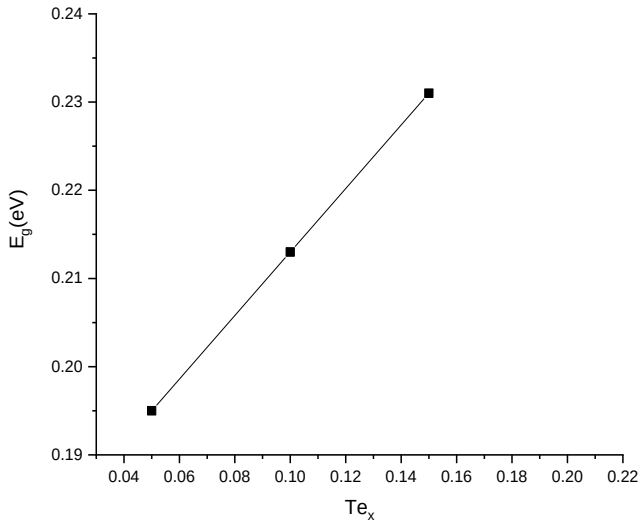

Figure 4.5: Plot of Band GapE_g V/s Te_x

4.3 Hall measurements:

An important characteristic that determines whether a material is metallic, semiconductive or insulating is its electrical property. According to this definition, semiconductors have an electric conductivity that lies between that of insulators and metals. A few examples of electrical properties are electrical resistivity, Hall coefficient, carrier densitiy, carrier types, Hall mobility, magneto-resistance and thermoelectricity.

The most frequent characterisation approach used to analyse electrical properties such as carrier mobility and impurity concentration is Hall measurements. Hall data can also be used to determine the electrically produced active impurities in a semiconductor. The nature of the charge carriers can be determined. The Van der Pauw [15, 16] approach was used for carrying out on Hall measurements.

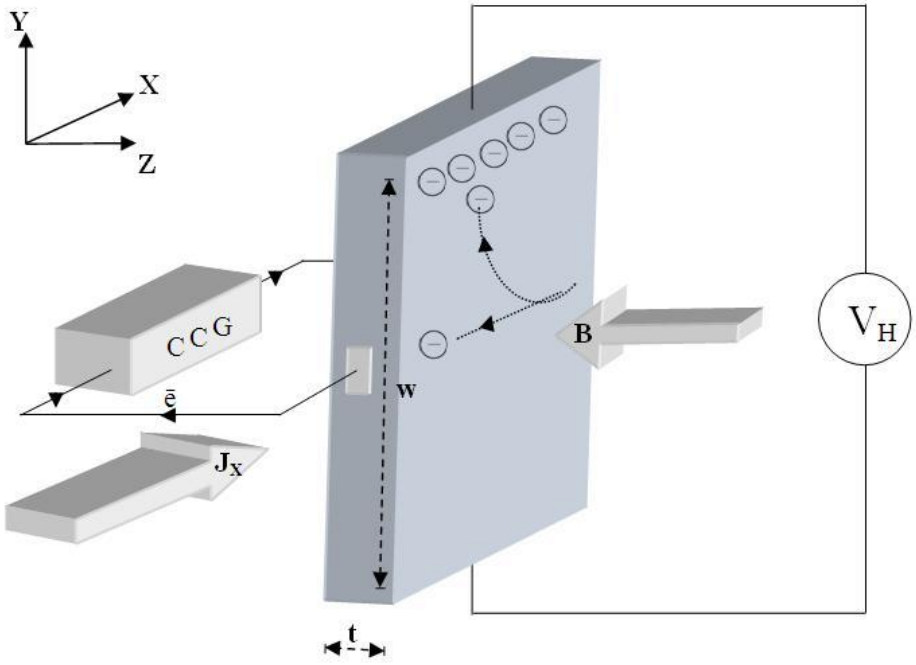

Figure 4.6: Schematic representation of Hall Effect in a conductor.

CCG – Constant Current Generator, J_X – current density

ē – electron, B – applied magnetic field

t – thickness, w – width

V_H – Hall voltage

Experimental Discussion:

The Hall measurements were carried out at room temperature using the Van der Pauw method. Two opposite probes were connected to a power supply with a digital current meter in series and across the other two probes; a digital micro voltmeter was connected to measure the voltage. The crystal was placed between the poles of a strong electromagnet giving a field of about 18K gauss maximum. The current and voltage were measured with and without the magnetic field. A large number of samples were measured at room temperature. The values of the Hall parameters including resistivity, carrier concentration, Hall coefficient and mobility for all the samples have been analysed. From analysis of the Hall parameters, the negative values of Hall- coefficient clearly point out the n-type semiconductor nature of $InBi_{1-x}Te_x$ (x= 0.05, 0.10, 0.15,) crystals with the majority charge carriers as electrons and all of them remain n-type in nature [17, 18]. From the value of resistivity and Hall coefficient the Hall mobility can be calculated using the equation,

$$\mu_H = |RH| / \rho_{av} \text{----(4.4)}$$

The effective charge carrier concentrations can be calculated ~~by~~ using the formula,

$$\eta_e = 1/ R_H\, e \text{ -----(4.5)}$$

The resistivity, carrier concentration, Hall coefficient and mobility of $InBi_{1-x}Te_x$ (x= 0.05, 0.10 and 0.15) are listed in Table-4.3.

Table 4.3 Hall Co-efficient, Carrier concentration, Resistivity for $InBi_{1-x}Te_x$ Crystal

Samples	Hall Coefficient R_H (Ωm /T)	Carrier concentration n(m^{-3})	Resistivity ρ (Ω m)
InBi	0.6626 x10^{-6}	9.432x10^{24}	.2290 x10^{-6}
$InBi_{0.95}Te_{0.05}$	1.1902 x10^{-6}	5.251x x10^{24}	.4961 x10^{-6}
$InBi_{0.90}Te_{0.10}$	3.13 x10^{-6}	1.996 x10^{24}	1.088 x10^{-6}
$InBi_{.085}Te_{.015}$	7.85 x10^{-6}	0.796 x10^{24}	2.72 x10^{-6}

4.4 Thermo electric measurement:

Energy conversion methods have constituted a significant part of the nation's research and development efforts in recent years. In the present day, thermoelectricity, thermionics, fuel cells, and magneto hydrodynamics are known to be the most advanced schemes. Future energy production will most likely involve each of these forms. Bismuth telluride-based alloys are among the most promising thermoelectric materials available today, not only because they are among the best thermoelectric materials near room temperature, but also because they can be prepared in many ways to improve their ZT values.[19-21]

$InBi_{1-x}Te_x$ has narrow band gap with large value of charge mobility in addition to reduced lattice thermal conductivity. Hence it may potentially find application as n-type thermo element. Many reports have mentioned about the theoretical prediction about bismuth and its related alloys as promising candidate for low dimension TE materials at 100 K[22,23].

Figure 4.7 shows the experimental set up used for studying the thermoelectric power (TEP). A temperature controller coil, made up of manganin wire, is used for measuring TEP by creating a desired temperature gradient between the copper block and the coil. Samples are placed between copper blocks. A freshly cleaved crystal plane along (001) direction was prepared for the experiment, having thickness of about 1-3 mm in order to maintain the required temperature gradient and also the distance between the copper blocks. Calibrated thermocouple pairs made up of Au-Fe (7%) - Chromel were used to measure the temperature gradient. The potential difference generated across the two Cu blocks is measured. A single voltmeter having accuracy of a nano volt was attached to measure the voltage.

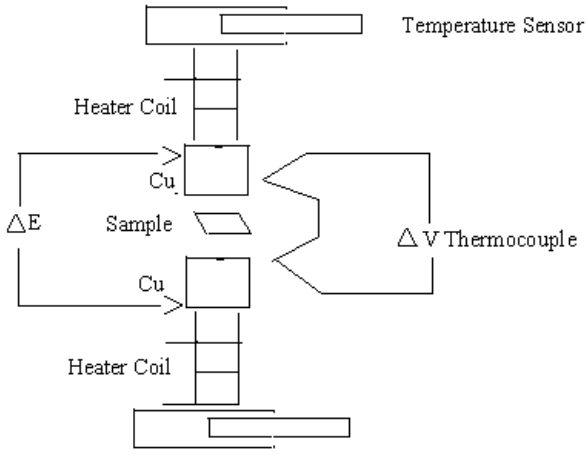

Figure 4.7: Block diagram of sample holder of TEP set up

Experimental Discussion:

The thermoelectric power can be defined as follows: if ΔT is the temperature difference across the sample and ΔV is the resultant potential difference this temperature gradient generates,

$$S = \Delta V / \Delta T \text{------(4.6)}$$

Due to the movement of electrons from hot end to cold end to minimize their energy, there will be an electric field developed across the conductor. As long as a temperature gradient exists between two ends of the sample, the thermoelectric voltage will be proportional to it. When a load is connected to the sample, the electric power is consumed by the load. Here the thermoelectric power corresponds to the electromotive force and the resistivity corresponds to the internal resistance. Maintenance-free electric power generation, waste heat energy recovery and long operating lifetime are some of the advantages of thermoelectric power generation.

The figures 8-10 show the TEP for the $InBi_{1-x}Te_x$ (x = 0.05, 0.10 and 0.15) crystals are plotted as functions of temperature between 300 to 400 K. It is clear that the addition of Te into InBi affects the TEP value.

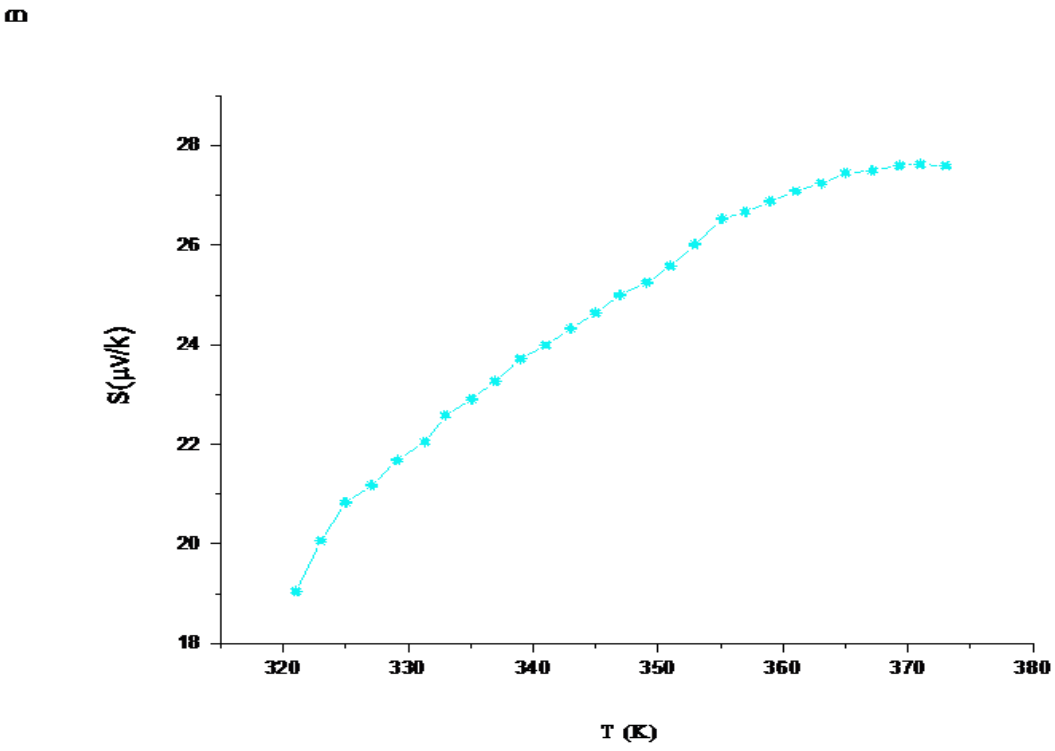

Figure 4.8: Plot of S (thermo emf) vs T (temperature) for $InBi_{0.95}Te_{0.05}$ crystal

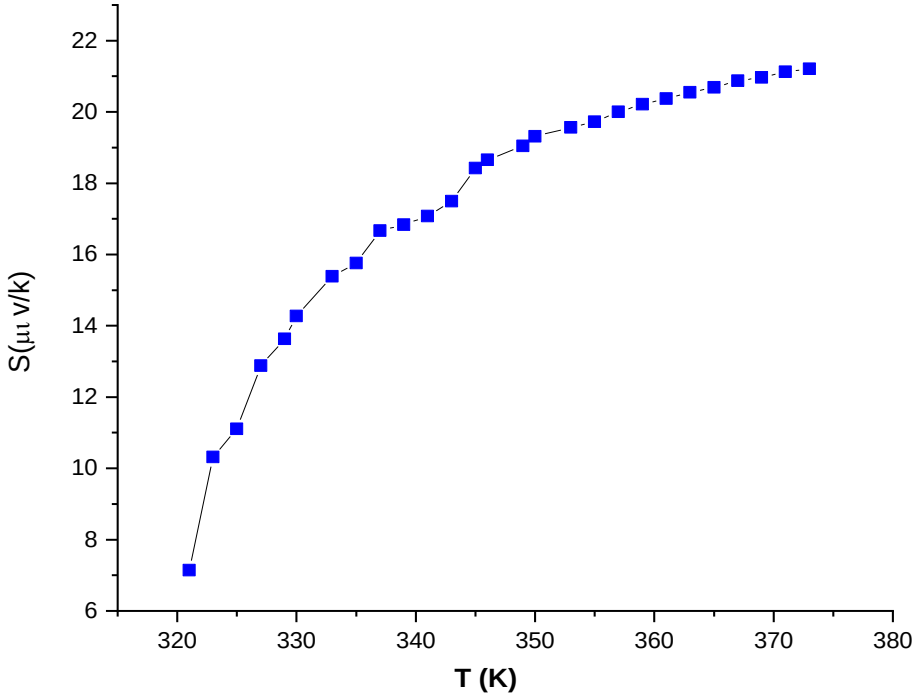

Figure 4.9: Plot of S (thermo emf) vs T (temperature) for $InBi_{0.90}Te_{0.10}$ crystal

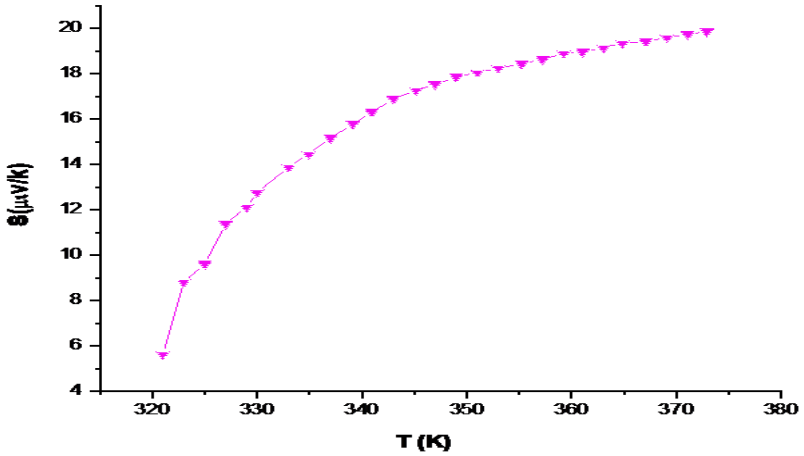

Figure 4.10: Plot of S (thermo emf) vs T (temperature) for $InBi_{0.85}Te_{0.15}$ crystal

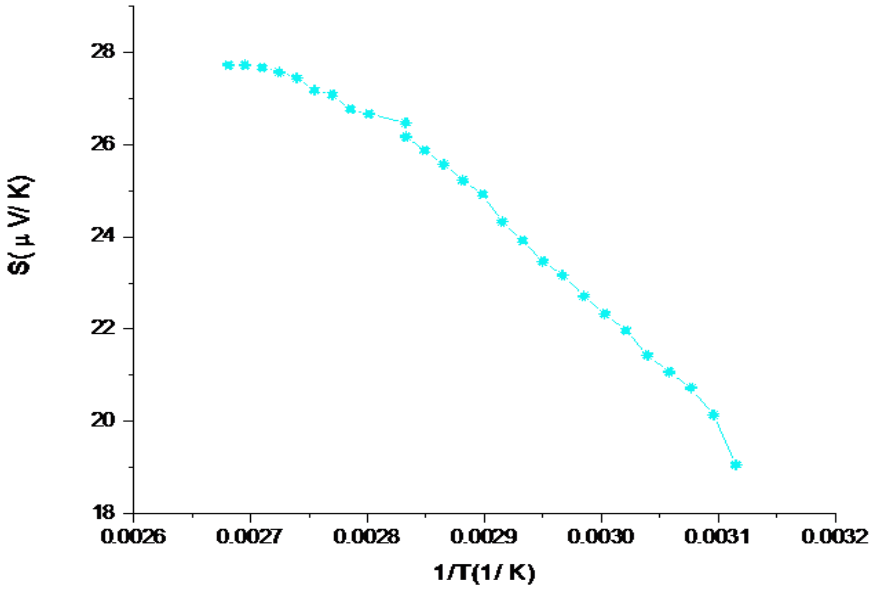

Figure 4.11: Plot of S (thermo emf) vs 1/T for $InBi_{0.95}Te_{0.05}$ crystal

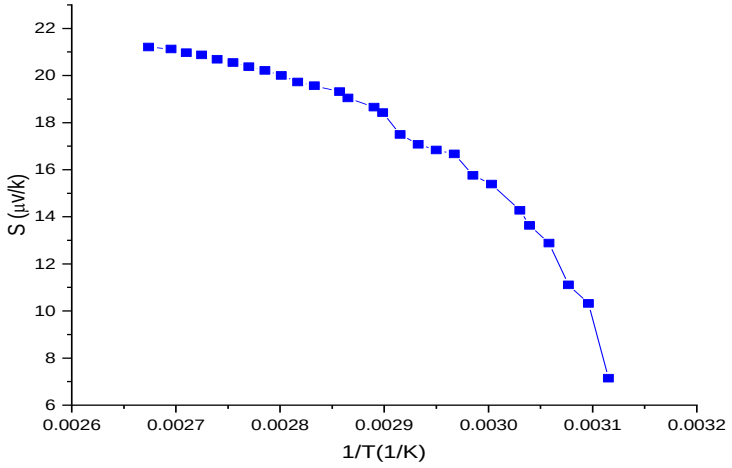

Figure 4.12: Plot of S (thermo emf) vs 1/T for $InBi_{0.90}Te_{0.10}$ crystal

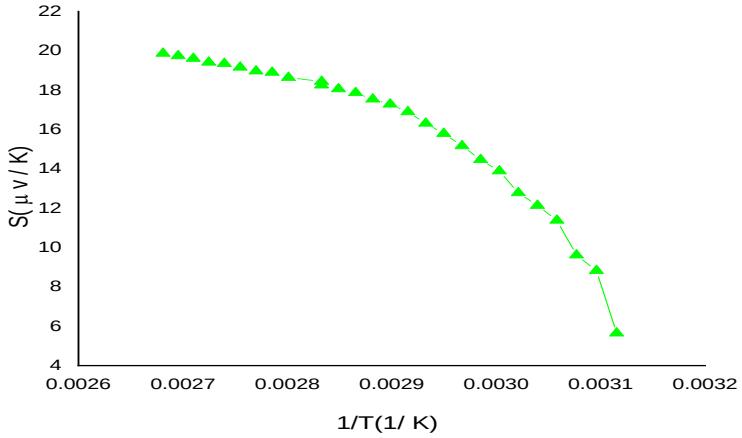

Figure 4.13: Plot of S (thermo emf) vs 1/T for $InBi_{0.85}Te_{0.15}$ crystal

The net TEP for any thermoelectric material having presence of both electron and holes, may be modeled by the relation,

$$S= (\sigma_e S_e + \sigma_p S_p)/ (\sigma_e +\sigma_p)$$

where σ_e and σ_p are the electrical conductivities and S_e and S_p are the TEPs for electrons and holes, respectively. Negative TEP values were observed implying higher mobility for electrons than for holes. The value of the TEP increases with decreasing temperature over a range of certain temperature. This raise is owed to the freezing-out of electrons and holes.

The variation of '*S*' of $InBi_{1-x}Te_x$ (x = 0.05, 0.10 and 0.15) crystals at different temperatures is shown in Figures 4.8- 4.10. The TEP is observed to be negative for $InBi_{1-x}Te_x$ (x = 0.05, 0.10 and 0.15) crystals over the entire temperature range revealing n-type semiconductor nature of all the samples.

An expression can be used to examine the temperature dependence of thermoelectric power in semiconductors given by Perluzzo et al. [24-26]:

$$\boldsymbol{S = -k/e[A + \frac{EF}{KT}]} \quad \text{----- (4.7)}$$

where *k* is the Boltzmann constant, e is the electronic charge, E_F is the energy separation of the Fermi level from the top of the valence band, A = ((5/2) - s) is the constant that varies from 0 to 4, which is affected by the dominant scattering process and may be understood to be a measure of the kinetic energy transported by carriers. The carrier concentration of the crystals essentially depends upon E_F.

There is a direct relation between E_F and the carrier concentration of the crystals. When plotting the TEP against the reciprocal of temperature (1/T), a straight line should be observed for small temperature ranges where E_F is fairly constant. Depending on whether electrons or

holes dominate the charge carriers in semiconductors, TEP has a different sign. The fact that TEP in $InBi_{1-x}Te_x$ (x = 0.05, 0.10 and 0.15) is negative clearly indicates that these crystals are n-type semiconductors.

Figures 4.11-4.13 shows the variation of TEP with the inverse of temperature for $InBi_{1-x}Te_x$ (x = 0.05, 0.10, and 0.15) crystals. The values of E_F and A obtained from the slope and intercept of the plots are listed in Table 4.2. [27-32]

where N_A is the effective density of states and is given by

$$N_A=2(2\pi m_e{*}kT)^{3/2}\text{--------}(4.8)$$

where m_e* is the effective mass of electrons. The values of carrier concentration obtained from Hall effect measurements (Table 4.3), the effective density of states N_A for all the crystals can be calculated with the help of the below formula,

$$n = N_A \exp (E_F/kT)\ \text{------}(4.9)$$

where E_F is the Fermi energy, k is the Boltzmann constant and T is the temperature. The values of effective density of states thus obtained are presented in Table 4.4. The effective density of states of electrons decreases with increase of Tellurium content in InBi.

Table 4.4: Effective Density of States and Fermi energy value of $InBi_{1-x}Te_x$ crystal

Crystals	E_F (eV)	N_A (m)$^{-3}$	A	S
$InBi_{0.95}Te_{0.05}$	0.023	$1.24x10^{25}$	1.078	1.43
$InBi_{0.90}Te_{0.10}$	0.030	$1.03\ x10^{25}$	1.30	1.2
$InBi_{.085}Te_{.015}$	0.035	$0.94\ x10^{25}$	1.36	1.14

.

4.5 Conclusions:

- There are no observable indirect transitions in the crystals. The band gaps of $InBi_{1-x}Te_x$ (x= 0.05, 0.10, 0.15) are about 0.195, 0.213 and 0.232 eV (all direct), respectively.
- The negative sign of Hall coefficient and thermal EMF show that all the crystals are of n-type having carrier concentration of 10^{24} m^{-3}, respectively.
- The Fermi energy of $InBi_{1-x}Te_x$ (x= 0.05, 0.10, 0.15) is about 0.023, 0.030 and 0.035, respectively.

References:

[1] Heavens O. S.,Optical properties of thin solid films, Butter Worths, London, (1955).

[2] Heavens O. S., Rept. Progr. Physics 23 (1960) 1.

[3] Bering P. H., Physics of thin films, Academic press, New York (1964) 69.

[4] Bennett H. E., BennettinJ. M.: Physics of thin films, Academic press, New York 4 (1967)

[5] S. M. Sze: Physics of Semiconductor devices: Wiley eastern limited New Delhi. (1979)

[6] Ajayakumar C. J., Kunjomana A. G., J. Mater Sci: Mater Electron (2016) 27,7467

[7] R. Tovar Barradas, C. Rincon, J. Genzalez, G. Sancher Pertez, Journal of and Chemistry of Solids 45 (1984) 1185.

[8] Eva C. Freeman, William Paul, Physical Review B 20 (1979) 716.

[9] J. Mendolia, D. Lemone, Physica Status Solidi (a) 97 (1986) 601.

[10] Soni P.H., Bhavsar S.R., Desai C.F., Pandya G.R. Journal of Crystal Growth, 340 (2012) 98.

[11] Berding M. A., Sher A., Chen A. B. and Miller W. E., Journal of Applied Physics Vol. 63 No. 1 (1988) 107.

[12] Premila Mohan, S. Moorthy Babu, P. Santhanaraghavan, P. Ramasamy, Materials Chemistry and Physics 66 (2000) 17

[13] Dey K. K., Banerjee D. and Bhattacharya R., Fizika A., (2002) vol. 11, No. 1, 153.

[14] Shah Dimple, Pandya Girish , Vyas Sandip , Jani Maunik , Jariwala Bhakti, Journal of Crystal Growth 312 (2010)

[15] Van der Pauw L. J. Philips. Res., (1958) 1.

[16] V. K. Dil, Bansal Bhavosh, Venkataraman V., Bhat H. L., Subbanna G. N. Applied Physics Letters 81, (2002) 1630.

[17] Lee J. J., Razeghi M., Opto Electronics Review 6(1), (1998) 25-36.

[18] Jani Maunik P., Ph.D. Thesis, M. S. Univ. of Baroda, (2007).

[19] Zhou Yan-fei, LIN Xiao-ya, BAI Sheng-qiang, et al. Journal of Crystal Growth, (2010), 312,775.

[20] Caoy q, Zhao X B, Zhu T J, et al. Applied Physics Letters, (2008), 92,143106.

[21] Di LI, Rui-rui Sun, Xiao-ying Qin, Material International 21(2011) 336-340.

[22] Katsuhiko Nishimura, Takayuki Yasukawa, Katsunori Mori, Physica B (2003) 1399-1400.

[23] Kavei G. (Material and Energy Research Centre, Tehran, Iran.

[24] PerluzzoG., Lakhani A. A., S. Jandl., Solid State Communications, **35**, (1980) 301.

[25] GoldsmidH.J., Application in thermo electricity, Methuen Monograph, London (1950)

[26] Solanki G. K. ,Gujarathi D. N., Cryst. Res. Technoi, Vol. 43, No2, (2008) 179-185.

[27] Mohanchandra K. P. &Uchil J., Thin solid films, 305 1997.

[28] Khan Zishan H., M zulfequar, Acta Physica Polonica A, Vol. 98(2000).

[29] Singh J. P., Master, J. Sci. Mater. Electron 2,105 (1995).

[30] Hicks W. T., J. Electrochem, Soc.111, 1058 (1964).

[31] Rahman M. A., Ashraf I. M., J. Phys. D 31,889 (1998).

[32] Zoater M., Conan A., Delaunay D., Phys. Stat. Sol.(a) 41,629 (1977).